EEG based over-complete rational dilation wavelet transform coupled with autoregressive for motor imagery classification

Hadi Ratham Al Ghayab [a], Yan Li [c], Mohammed Diykh [b,e,*] , Aqeel Sahi [c] ,
Shahab Abdulla [d], Ahmed Rashid Alkhuwaylidee [f]

[a] Faculty of Business and IT, TAFE Queensland Southwest, QLD 4350, Australia
[b] University of Thi-Qar, Nasiriyah, College of Education for Pure Science, 64001, Iraq
[c] School of Mathematics, Physics and Computing, University of Southern Queensland, QLD 4350, Australia
[d] UniSQ College, University of Southern Queensland, QLD 4350, Australia
[e] Information and Communication Technology Research Group, Scientific Research Centre, Al-Ayen University, Thi-Qar, 64001, Iraq
[f] University of Thi-Qar, College of Computer Science and and Mathematics, Department of Information Technlogy, 64001, Iraq

A B S T R A C T

Motor Imagery (MI) based Brain-Computer Interface (BCI) applications are designed to analyse how the brain interacts with the external environment from electroencephalograph (EEG) signals. Despite current models achieving promising results, developing an accurate classification of MI from EEG signals remains a significant challenge. In this paper, we designed an MI classification model named (ORDWT_AR) utilising an over-complete rational dilation wavelet transform (ORDWT) coupled with an autoregressive (AR) model. Firstly, EEG recordings are segmented into intervals using a sliding window method. Then, each EEG segment is passed through the ORDWT to analyse EEG signals. As a result, a series of stop bands is obtained from each segment. Then, the AR is adopted and integrated with ORDWT to extract representative features from each EEG interval. The selected features are sent into several classification models, including Weighted k-nearest Neighbour (WKNN), Decision Tree (DTree) and Boosted Trees (BST). Four benchmark EEG databases were used to evaluate the proposed model, three of which were collected from brain-computer interface (BCI) Competition III and one from the CHB-MIT. The results demonstrated that the proposed model ORDWT_AR coupled with the WKNN classifier achieved an average of 99.8% classification accuracy for the three BCI competition III datasets and 99.7% for the CHB-MIT dataset. The obtained results revealed that the proposed scheme is a promising tool for classifying EEG signals and has outstanding results. The proposed model can support experts in aiding disabled people to interact with their environment accurately and improve the quality of their lives.

1. Introduction

The human brain is the most critical organ, controlling all body activities. For example, when a subject moves or does something, the brain cells are catalysed and send electrical signals to a specific body part to respond appropriately (Wolpaw et al., 2002, Ang et al., 2015). To reflect the correct response, various signals could be involved, including Electroencephalography (EEG), Electrooculography (EOG), Electrocardiogram (ECG), and Electromyography (EMG) (Nguyen et al., 2015, Zhang et al., 2017, Gaur et al., 2018).

The BCI system is a communication system that transfers neuronal

information to commands that are employed to control external devices (Gaur et al., 2018, Dose et al., 2018). BCI systems can provide a promising communication channel for patients with physical injuries and impaired movements through various techniques (Siuly et al., 2010). BCI systems are designed based on several techniques named magnetoencephalography (MEG), positron emission tomography (PET), functional magnetic resonance imaging (fMRI), and optical imaging. EEG favours those tools, as PET, FMRI, and MEG are technically expensive and depend on blood flow, which requires a long time to be collected and analysed (Wolpaw et al., 2002). For most medical applications, EEG signals have become the most frequent diagnostic tool used to study the

brain due to their portability, low cost, pain-free monitoring solution and real-time capabilities.

In the recent decade, several attempts based on Wavelet Transform (WT), Short-Time Fourier Transform (STFT), Discrete Wavelet Transforms (DWT), and Empirical Mode Decomposition (EMD) have been made to classify MI EEG signals (Venkatachalam et al., 2020). Although those models have achieved promising results, they suffer from some issues. For example, WT does not work correctly with non-stationary signals, such as EEG signals, and it becomes computationally intensive (Rai et al., 2007), DWT causes low oscillations and severe oscillation frequency, which weakens the ability of the DWT to match high oscillatory features (Chen et al., 2012). With STFT, the window size is the same for all frequencies, while EEG signals require a more flexible tool with different window sizes depending on the signals' characteristics (Kwok and Jones, 2000). In addition, EEG signals produce periodical impulses and amplitude frequency modulation contents. Designing an accurate model to analyse EEG patterns is essential for a BCI system to extract the most representative features from MI signals recorded via EEG.

Rational Dilation Wavelet Transformed (RDWT) has recently been widely used in different fields. It was developed to enhance the limitation of dyadic WT and EMD. The RDWT technique can adjust the frequency resolution. However, it neglects to consider the oscillation property of its wavelet functions (Chen et al., 2012).

Deep learning and graph-based approaches have recently been widely used in MI EEG classification. For example, Chatterjee et al. applied an adaptive autoregressive feature extraction model to classify motor imagery EEG signal classification (Chatterjee et al., (2019). Chunduri et al. suggested a multi-scale spatiotemporal self-attention (SA) network model to extract representative features from EEG signals (Chunduri et al., 2024). Their model utilised temporal and spatial features of EEG to classify motor imagination EEG segments into four classes. Meng et al. adopted a time-domain and frequency-domain feature-based model (Meng et al., 2021). The extracted features were used as inputs into a neural network. Ma et al. designed a multi-branch graph adaptive network model for imagery EEG signal classification (Ma et al., 2023). In that study, the relevant model branch-based adaptive technique was employed in the classification phase. (Wang et al. 2022) employed a graph embedding method in which the time-domain features were attained using a convoluting technique. (Pan et al. 2024) integrated principal components analysis, kernel principal components analysis and spectral density to extract EEG features. Several classification models were employed to classify EEG features, such as the extreme learning machine, k-nearest neighbour, light, and gradient boosting machine support vector machine. (Venkatachalam et al. 2020) presented a hybrid approach that utilised Kernel Extreme Learning Machine, Principal Component Analysis and Fisher's Linear Discriminant. Different EEG features were pulled out and sent to several machine-learning models. (Fei and Chu, 2022) applied a hybrid model to classify EEG signals. They combined singular value decomposition, wavelet transform, phase space reconstruction and multi-layer twin support vector machine. (Han et al., 2022) employed a deep learning model for motor imagery EEG classification. In that study, a parallel convolutional neural network model was proposed to classify motor imagery signals. (Ma et al., 2022) designed an end-to-end novel multi-branch hybrid neural network model for EEG motor imagery classification. They divided EEG signals into four frequency bands and employed a Bidirectional Gated Recurrent Unit (BGRU) to extract EEG features from EEG frequencies.

As EEG signals exhibit various oscillatory behaviours (low and high oscillations), most of the developed models depend on nonlinear characteristics analysis, which does not work correctly with EEG behaviours. Consequently, this research provides a novel technique to accurately analyse and classify the MI classification model. In this paper, an ME classification model named ORDWT_AR is proposed. The proposed model combines the over-complete RDWT (ORDWT) and an

Table 1
Dataset used for model evaluation.

Dataset	Number of subjects
Data set IVa	5
Data set V	3
BCI Competition III	3
CHB-MIT EEG	22
Total number of subjects	33

autoregressive (AR) model. Combining ORDWT and OR can produce good frequency resolution and representation for EEG signals. The proposed model has more flexibility in removing redundant frequencies in the signals. Furthermore, the proposed model was designed to be effective to apply to different EEG data. In this paper, epileptic and motor imagery EEG signals were used to validate the proposed mode. The results demonstrated the proposed model had the ability to analyse and classify these tow signals Three prevalent classifiers, weighted k-nearest Neighbour (WKNN), decision tree (DTree), and boosted trees (BST), are adopted to classify the extracted features into various MI tasks. The proposed model was assessed using four publicly available datasets. The main contributions of this study are as follows:

- We proposed an MI recognition method based on EEG signals. The proposed model efficiently addressed the issue of low oscillations associated with classic decomposition models for analysing EEG using over-complete RDWT.
- The proposed model combined over-complete RDWT (ORDWT) and an autoregressive (AR) model to benefit from both methods. The proposed hybrid model seeks to improve ME classification accuracy and channel selection.
- We validated the effectiveness of the proposed method using four publicly available EEG datasets, and the results obtained demonstrated the proposed model's superiority to other methodologies.

This paper is organised as follows: Section 2 explains the data description, the proposed algorithm, and performance measurements. Section 3 provides the experimental results. Section 4 presents the main findings and a comparative study report with several existing methods. Section 5 concludes and suggests future work.

2. Material and methods

2.1. EEG datasets description

All four datasets used in this study are publicly available. The EEG datasets were collected during motor and mental imagery tasks and scalp epileptic EEG data. As shown in Table 1 (Shoeb, 2009), 33 subjects were considered in this paper.

1. The IVa datasets in BCI Competition III were collected from five healthy people and denoted as aa, al, av, aw, and ay (Blankertz et al., 2006). Each subject was tested with two motor imagery (MI) tasks (two classes). Class number one is for the right hand and is labelled as RH. Class number two is for the right foot and is labelled as RF. All the datasets were recorded when the subjects sat in a comfortable chair and rested their arms on armrests, and 118 electrodes were used to record the EEG signals. There were 280 cues for each of the five subjects (aa, al, av, aw, and ay). Through the recording task, the volunteer was required to perform either of the two MI tasks (RH and RF). Each EEG recording is 3.5 s in duration.
2. The V EEG datasets from BCI Competition III were recorded from three health subjects and denoted as subj1, subj2, and subj3. The subjects were without any previous experience with BCI or mental training (Millan et al., 2004). The subjects participated in three consecutive days of recording. Each subject was tested with three
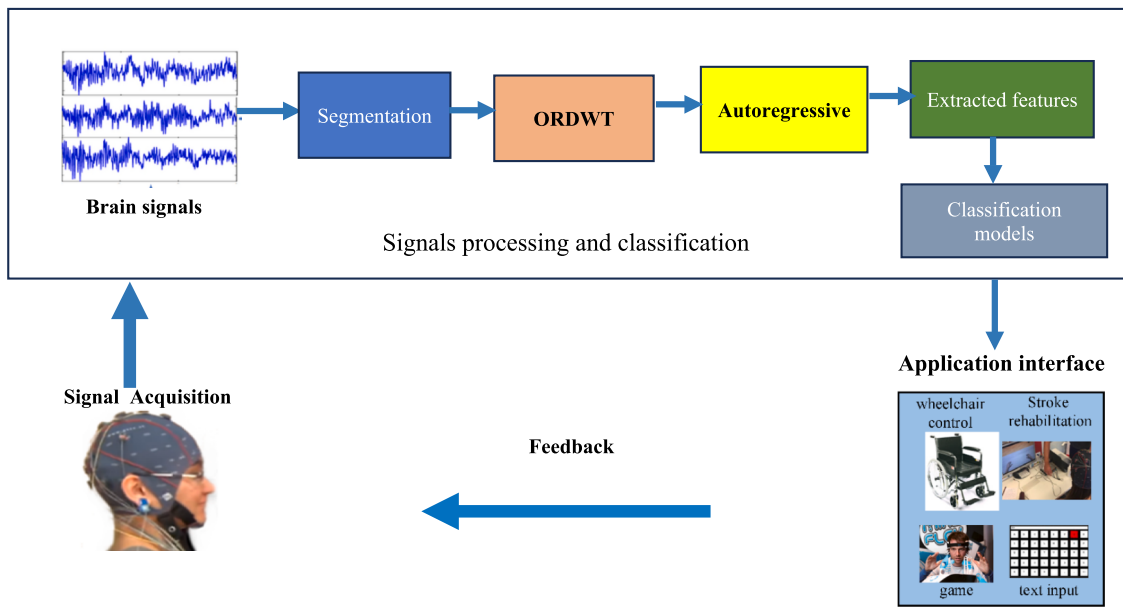
Fig. 1. Diagram of the proposed technique for MI EEG classification.

mental imagery (MenI) tasks (three classes). The first class was for the left hand and was labelled as LH. The second class was for the right hand and labelled RH, while the third class was for generating words beginning with the same random letter and labelled W. On each day of MenI tasks, subjects did several consecutive four-minute recording sessions with more than 5 min breaks between those sessions. During each training session, the subjects switched randomly every 20 s between the three MenI tasks.

3. The IIIa EEG datasets from BCI competition III were recorded from three volunteers. Each person sat in a comfortable chair with armrests and was tested with four random imagery tasks of four classes, such as left hand, right hand, foot or tongue, according to a cue. These tasks are labelled as LH, RH, F, and T. The multi-class EEG was sampled at 250 Hz and filtered between 1 and 50 Hz with a Notch filter. The IIIa datasets recorded from a 64-channel amplifier from Neuroscan contain 60 channels of EEGs (Lotte et al., 2010).

4. The CHB-MIT EEG datasets are freely available online (Shoeb et al., 2022). In this study, the EEG data were collected from 22 patients using 22 electrodes and utilising 10–20 EEG systems. These datasets were recorded at a 256 Hz sampling rate with 16-bit resolution. Five patients had less than 10 seizures a day, and ages between 10 and 14 were selected for EEG classification.

2.2. Proposed technique

This section provides a detailed description of the proposed technique. The diagram of the proposed ORDWT_AR method is shown in Fig. 1. EEGs are considered vital tools in BCI systems to determine the mental state of patients, response to actions, and cognitive state changes. In this paper, we designed an intelligent model for ME classification. The EEG data were collected from public datasets. Each EEG signal is segmented into intervals using a sliding window technique. Then, each EEG segment is passed through ORDWT. AR is integrated with ORDWT. The AR was employed to extract the most representative features from EEG signals. The extracted features are sent to several classification models named WKNN, DTree and Boosted Trees (BST). Several evaluation metrics are used to evaluate the proposed model.

2.2.1. Pre-processing and feature extraction

In this study, feature extraction is used to reduce the dimensionality of EEG signals and remove redundant and irrelevant information. The extracted data are utilised to make the whole classification procedure faster and more accurate than the entire EEG data. This subsection illustrates the feature extraction procedure.

2.2.1.1. Segmentation. EEG signals are non-stationary, oscillating and contain many redundant data (Alsafy and Diykh, 2022, Lafta et al., 2018, Al-Hadeethi et al., 2021, Abdulla et al., 2023, Diykh et al., 2023, Mohammed et al., 2023). A segmentation approach is used to partition each EEG signal into smaller segments called windows, denoted as Wi, to make EEG signals close to quasi-stationary. Eq. (1) shows how to determine the window size empirically.

$$W_{size} = S(x)/W_i; i = 1, \cdots n \tag{1}$$

where W_{size} refers to the window size; $S(x)$ is the input signal of each class; i is the number of windows. In this paper, the MI EEG data from each class are divided into four windows ($i = 4$).

2.2.1.2. Over-complete rational dilation wavelet transform (ORDWT). This study employs the technique ORDWT to decompose each MI EEG signal (Bayram and Selesnick, 2009, Bayram et al., 2007). The ORDWT has several advantages over the classic transformation technique. First, each frequency scale produced by ORDWT is characterised by a number of signals generated by different bandpass filters. Second, its construction involves polynomial array spectral factorisation which is straightforward in principle than other frequency-domain approaches. As a result, it can be produced good frequency resolution. Third, it has more flexibility in the repetition factor of the transform.

The ORDWT depends on a diversity of controlling parameters, such as polyphase components (p), quality factor (q) and redundancy (r). Like other WTs, the ORDWT is executed using two-channel filter banks. The dilation factor of the ORDWT depends on the rational value of q/p, with the condition of $q > p$. In this study, we set the dilation factor as $1 < q/p < 2$. The scaling and wavelet functions in the ORDWT depend on the rational dilation scaling relation, as shown in Eq.2 and Eq.3.

$$\varphi(t) = \left(\frac{q}{p}\right)^{1/2} \sum_{m \in Z}^{1} h_0(m) \varphi\left(\frac{q}{p}t - m\right) \tag{2}$$

$$\psi(t) = \left(\frac{q}{p}\right)^{1/2} \sum_{m \in Z}^{1} h_1(m) \psi\left(\frac{q}{p}t - m\right) \tag{3}$$
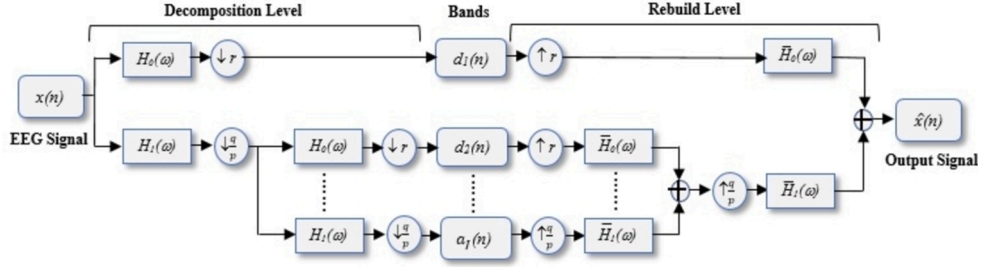
Fig. 2. The ORDWT decomposes the input EEG signal ($x(n)$) into stop band $H_0(\omega)$ and low pass band $H_1(\omega)$ at j^{th} levels and rebuilds the decomposed $\hat{x}(n)$.
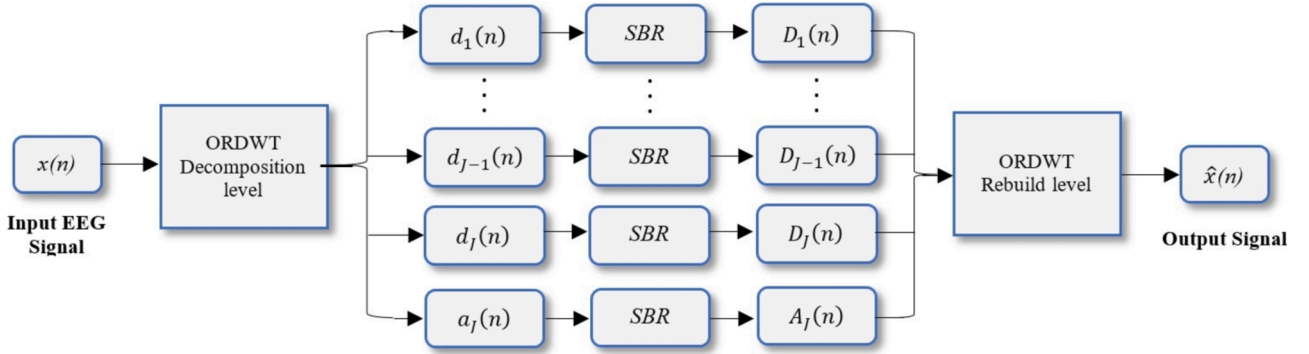

Fig. 3. Rebuild all the wavelet bands from stop and low pass series through using the single branch reconstruction (SBR).

where $\varphi(t)$ is the scaling function. $\psi(t)$ is the wavelet function $.h_0(m)$ is a scaling function filter, and $h_1(m)$ is the wavelet function filter. The ORDWT decomposes EEG signals into different levels of decomposition based on p, q and r parameters.

The EEG signal is decomposed into stop and low pass bands at each level. The functions of $H_0(\omega)$ and $H_1(\omega)$ are the frequency responses of $h_0(n)$ and $h_1(n)$, respectively, as shown in Fig. 2. To calculate the frequency responses, $H_0(\omega)$ and $H_1(\omega)$ are defined as in Eq. (4) and Eq.5 (Bayram and Selesnick, 2009, Bayram and Selesnick, 2007).

$$H_0(\omega) = \begin{cases} \sqrt{pq}, \omega \in \left[0, \left(1-\dfrac{1}{r}\right)\dfrac{1}{p}\pi\right] \\ \sqrt{pq}\,\theta_{H_0}\left(\dfrac{\omega-a}{b}\right), \omega \in \left[\left(1-\dfrac{1}{r}\right)\dfrac{1}{p}\pi, \pi\right] \\ 0, \omega \in \left[\dfrac{1}{q}\pi, \pi\right] \end{cases} \quad (4)$$

$$H_1(\omega) = \begin{cases} 0, \omega \in \left[0, \left(1-\dfrac{1}{r}\right)\pi\right] \\ \sqrt{r}\,\theta_{H_1}\left(\dfrac{\omega-pa}{pb}\right), \omega \in \left[\dfrac{r-1}{r}\pi, \dfrac{p}{q}\pi\right] \\ \sqrt{r}, \omega \in \left[\dfrac{p}{q}\pi, \pi\right] \end{cases} \quad (5)$$

where a, b and θ are defined as:

$$a = \frac{\left(1-\frac{1}{r}\right)\pi}{p} \quad (6)$$

$$b = \frac{1}{q} - \frac{\left(1-\frac{1}{r}\right)1}{p} \quad (7)$$

$$\theta(\omega) = \frac{(1+cos(\omega))}{2}\sqrt{2-cos(\omega)}, for\,\omega \in [0, \pi] \quad (8)$$

Function $\theta(\omega)$ is utilised to build the stop and low pass bands of $H_0(\omega)$ and $H_1(\omega)$. $\theta(\omega)$ originates from the orthonormal of the Daubechies wavelet filters that include two vanishing moments. Although all orthonormal filters are usable for building any sharp edges, they cause a very slow decomposition rate of the $\varphi(t)$ and $\psi(t)$.

To rebuild the decomposed EEG signal and make the signals clear, the condition holds was checked for the ORDWT based on $|H_0(\omega/p)|^2/(pq) + |H_1(\omega)|^2/r = 1$. It indicates that $x(n) = \overline{x}(n)$ as shown in Fig. 2. The rebuilding procedures of the decomposed EEG signals are discussed as follows:

- The length of the stop band series is amputated as the decomposition proceeds. To regain the stop band's lengths, the single branch reconstruction (SBR) is used to rebuild the series of the decomposition levels into corresponding wavelet sub-band signals, as shown in Fig. 3.
- After decomposing the input EEG signal to the jth level and using the SBR, the EEG signal is rebuilt into the jth-1 level band, as shown in Figs. 2 and 3 according to Eq.9.

$$\overline{x}(n) = \left\{A_j(n), D_j(n), D_{j-1}(n), \cdots, D_1(n)\right\} \quad (9)$$

where $A_j(n)$ is the rebuild approximation sub-bands of the EEG signal $.D_j(n)$, $and D_{j-1}(n)$ refer to the jth rebuild sub-bands of the EEG signal.

- The functions, $\overline{H}_0(\omega)$ and $\overline{H}_1(\omega)$ are defined using Eq.10 and Eq.11, which are the frequency responses of $\overline{h}_0(n)$ and $\overline{h}_1(n)$, respectively.

$$\overline{H}_0(\omega) = \frac{1}{p}h_0\left(\frac{\omega}{p}\right) \quad (10)$$

$$\overline{H}_1(\omega) = h_1(\omega) \quad (11)$$

where $\overline{h}_0(n)$ and $\overline{h}_1(n)$ are utilised over the decomposition process. In
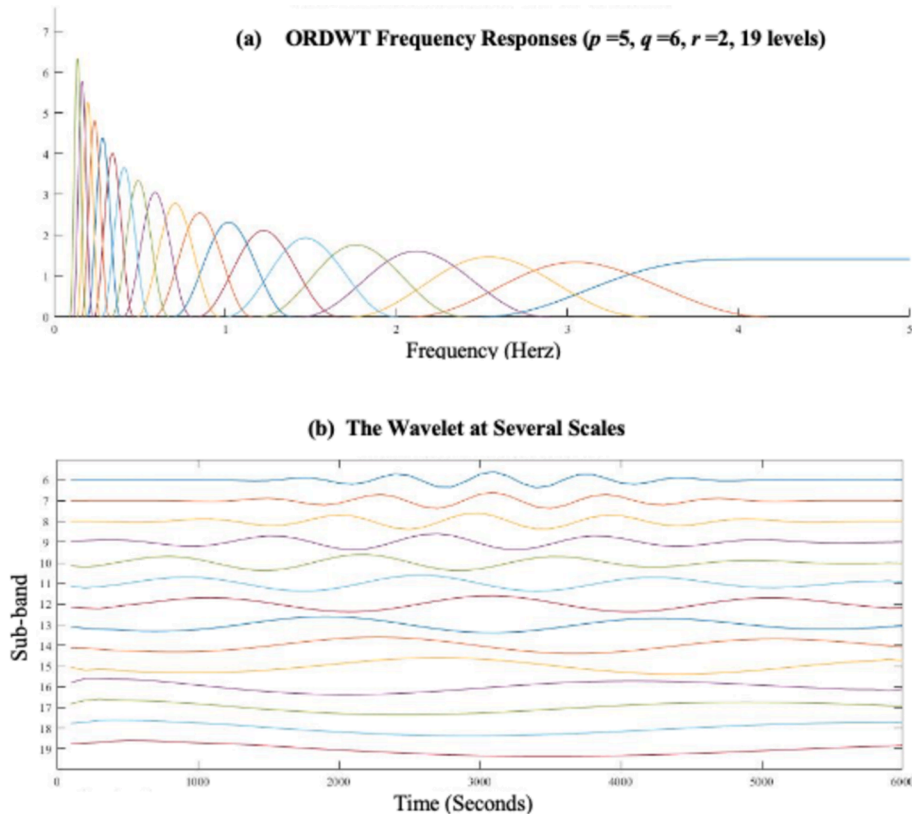
Fig. 4. Examples of ORDWT and ordinary WT decomposition: **(a)** ORDWT method **(b)** WT method.

addition, for the jth decomposition level, the frequency responses, $\overline{H}_0(\omega)$ and $\overline{H}_1(\omega)$, can be extended to:

$$\overline{H}_{0_j}(\omega) = \frac{1}{p_j}H_{0_j}\left(\frac{\omega}{p_j}\right), j \geq 1 \tag{12}$$

$$\overline{H}_{1_{j-1}}(\omega) = \begin{cases} H_1(\omega), j = 0 \\ \dfrac{1}{p_j}H_{0_j}\left(\dfrac{\omega}{p_j}\right)H_1\left(\left(\dfrac{q}{p}\right)^j \omega\right), j \geq 1 \end{cases} \tag{13}$$

where

Fig. 5. The accuracy results through R value selection by the AR technique using different EEG datasets from the BCI Competition III system. **(a)** IVa dataset, **(b)** V dataset, **(c)** IIIa dataset.

$$\overline{H}_{0j}(\omega) = \begin{cases} \prod_{n=0}^{j-1} H\left(q_{j-1-n}p_n\omega\right), \omega \in \left[0, \dfrac{\pi}{q_j}\right] \\ \\ 0, \omega \in \left[\dfrac{\pi}{q_j}, \pi\right] \end{cases}, j \geq 1 \qquad (14)$$

To rebuild the decomposed EEG signal based on the ORDWT method, the parameters of p, q and r should satisfy the allowable condition as below:

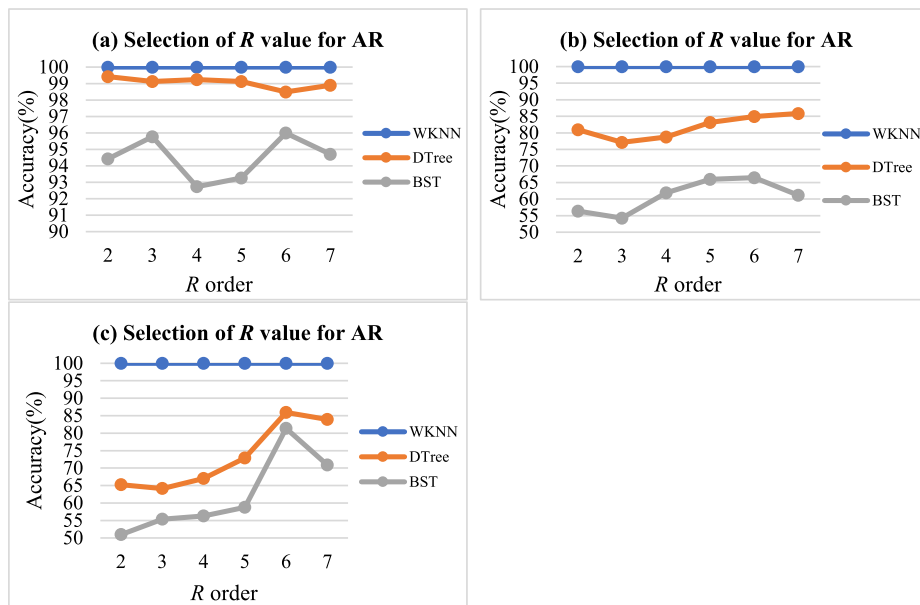$$\left(1 - \frac{1}{r}\right)\frac{1}{p}\pi\left\langle\frac{\pi}{q} \Rightarrow \frac{p}{q} + \frac{1}{r}\right\rangle 1 \qquad (15)$$

This condition does not allow the passbands to overlap between those bands. This study applies the proposed method to three datasets in BCI Competition III, as explained in Section 2.1. Also, p, q, and r were set empirically for both datasets at $p = 5$; $q = 6$; $r = 2$. In addition, the decomposition level (j^{th}) was also set empirically at 19. Fig. 4 presents a difference between ordinary WT and the proposed ORDWT techniques at level 19 of decomposition.

2.2.1.3. Autoregressive (AR) method. The AR method is a linear prediction method used to extract the most representative features and predict an output from the algorithm depending on the previous outputs. It is a parametric method for the power spectral density estimation (Ganapathy et al.,2014, Rajan and Rayner, 1996). The details of the AR method are explained in (Ganapathy et al.,2014). The AR method works based on the R value, which should be selected carefully. To choose a suitable R value, this study performs different R orders in the AR technique as shown in Fig. 5 (a), (b) and (c). The R value is selected as 6 for the results in Fig. 5.

2.2.1.4. Classification. The extracted features were taken from motor imagery (MI) EEG signals based on the BCI systems and forwarded to different classifiers, such as the WKNN, DTree, and BST, for performance comparisons. The following section explains the classifiers used in this study.

2.2.1.5. Weighted k-Nearest Neighbor (WKNN). The K-nearest neighbour classifier is one of the simplest methods among machine learning algorithms (Abdulla et al., 2023). It is the most popular nonparametric classifier. For instance, m data points are used as the input testing set to this classifier that finds the k nearest neighbours through the training set. In the WKNN, the classifier is used to weigh the class candidates. Furthermore, the similarity score for each nearest neighbour class to the test set is used as the weighted class. If the number of the nearest neighbours share different classes, the neighbour weights of this class are placed together. The sum of the resulting weights is utilised as the likelihood of this class concerning the test set. Here, a ranking list is found for the test set through the classifying scores of the candidate classes. The classification of the WKNN method can be defined as in equation (16).

$$SC(m, t_i) = \sum_{m_j \in WKNN(m)} S(m, m_j)C(m_j, t_i) \qquad (16)$$

where $SC(m, t_i)$ refers to the score of the m testing set and t_i is the training set. $S(m, m_j)$ indicates the similarity score of each nearest neighbour class. $WKNN(m)$ is the set of k nearest neighbours of input m file; $C(m_j, t_i)$ indicates the classification for m_j with relation to t_i training sets that can be defined as below:

$$C(m_j, t_i)\begin{cases} 1, m_j \in t_i \\ 0, m_j \notin t_i \end{cases} \qquad (17)$$

where m testing file should be assigned to the class that has the high scoring weighted sum. In this study, the number of the neighbours k is

Table 2
The number of samples in the training and testing sets used in this study.

Database	Case	Total	Training set	Testing set
IVa dataset	**RH** vs **RF**	5160	3440	1720
V dataset	**RH** vs **LH** vs **W**	4644	3096	1548
IIIa dataset	**RH** vs **LH** vs **F** vs **T**	39,216	26,144	13,072
CHB-MIT	**Normal** vs **Seizure**	58,824	39,216	19,608

selected at $k = 10$. The motivation for applying this classifier is that it efficiently minimises the fuss shown in the input data.

2.2.1.6. Decision tree (DTree). DTree is one of the most utilised machine learning techniques and was developed by (Kevric et al., 2017). The DTree method is structured as a tree containing internal (test sets) and leaf nodes (train sets). Each internal node represents a result of the test. Therefore, each terminal node (leaf node) has a class label that helps to make a decision. For more details on this method, readers may refer to. The main reason for applying the DTree classifier in this study is its easy use. There is no need for further knowledge or parameter setting, and the classification phase is simple and fast. In addition, the DTree can deal with multi-dimensional data.

2.2.1.7. Boosted trees (BST). The BST classifier is a powerful method. It is designed to classify features with high predictive possibility. This method describes the complex relationships between various features in a dataset by collecting numerous simple decision tree models. The classifier is based on a decision tree. The BST classifier often leads to significantly greater accuracy than competing machine learning methods, such as logistic regression, neural networks and support vector machines. However, the major limitation of the BST classifier is that it needs to build a large number of decision trees, which takes a long time during the training procedure and leads to difficulty optimising it. For details of this method, readers can refer to (She et al., 2018).

2.3. Performance measurements

In this study, different measurements were used to assess the performance of the proposed technique. The *f*-fold cross-validation method was used. The extracted features were partitioned into (*f*) folds or parts (Jin et al., 2019). In each exaction, two parts are used, with one serving as a testing set and the rest as the training set. Table 2 shows the number of features employed in the testing and training sets.

An overall accuracy rate (OAR) is calculated from the entire *f*-fold cross-validation procedure. In each implementation, 10- folds are used to test the classification called tests (T_1, T_2, ... T_n), and OAR is yielded through the 10-fold cross-validation technique.

For further investigation, each subject from the three datasets in the BCI Competition III was used as the testing set to validate the proposed method. For instance, one subject was taken as testing input, and the rest were utilised as the raining input to the classifier.

In addition, a number of statistical measures were applied to evaluate the proposed method's performance, such as accuracy (AC), positive predictive value (PPV), and negative predictive value (NPV). Their equations are given below (Selim et al., 2020, Al-Saadi et a.l, 2022, Diykh et al., 2021).

$$AC = \frac{true positives + true negatives}{total samples} \times 100 \qquad (18)$$

$$PPV = \frac{true positives}{total positives} \times 100 \qquad (19)$$

$$NPV = \frac{true negatives}{total negatives} \times 100 \qquad (20)$$

Table 3
Performance of the ORDWT_AR method for three MI EEG databases using 10-cross validation.

Database	Case	Classifier	AC (%)	PPV (%)	NPV (%)
IVa dataset	RH vs RF	WKNN	98	98	97
		DTree	97	96	97
		BST	94	95	92
V dataset	RH vs LH vs W	WKNN	99	98	99
		DTree	82	80	80
		BST	64	65	64
IIIa dataset	RH vs LH vs F vs T	WKNN	99	98	97
		DTree	74	73	74
		BST	65	64	63
CHB-MIT	**Normal** vs **Seizure**	WKNN	98	99	98
		DTree	97	96	97
		BST	96	95	94

3. Experimental results

The first goal of this research is to develop a novel technique for classifying EEG signals. To check the effectiveness of the proposed system, a set of experiments was conducted using three different BCI datasets and one epileptic dataset, as mentioned in Section 2.1. The ORDWT_AR was applied to analyse the signals, and the vital representative features from all datasets were obtained. This research used three steps to analyse EEG signals from the BCI Competition III and CHB-MIT. Firstly, the input EEG signals were partitioned into several segments called windows. After that, the ORDWT approach was applied for each window of the EEG recordings to decompose and rebuild the EEG data. In this paper, the Autoregressive (AR) method was adopted to reduce the dimensionality of the ORDWT coefficients and to extract patterns and key characteristics of EEG signals. Table 2 illustrates the number of samples how these samples were distributed between training and testing the proposed model. The extracted features were forwarded to the WKNN, DTree, and BST classifiers to select the most suitable classifier. The experiments were conducted using MATLAB R2018b on a computer with Intel (R) core i7-7700, 3.60 GHz CPU, RAM capacity of 16 GB. The proposed approach was tested and assessed through different evaluation measurements, as shown in Section 2.3.

The data from all subjects was divided into training and testing sets to ensure robust evaluation. The AC, PPV and NPV metrics were employed to evaluate the proposed ORDWT_AR technique. The 10-cross validation strategy was employed to calculate the results in Table 3. The AC rates of the ORDWT_AR with the WKNN classifier for three BCI Competition III and CHB-MIT datasets were 99 % and 98 %, respectively. The WKNN classifier scored the highest accuracies compared with the DTree and BST classifiers. On the other hand, the lowest

accuracies reached for all databases were 94 %, 64 %, 65 % and 96 %, respectively, by the BST classifier. The second-highest result was yielded by the DTree classifier, as shown in Table 3. The DTree classifier yielded an average of the PPV and NPV of 96 % and 97 %, respectively, for the IVa datasets, and PPV = 80 % and VNP = 80 % for the V datasets of the MI EEG signals. However, the proposed technique with DTree achieved PPV = 73 % and VNP = 74 % for IIIa datasets due to multiclass, which was the second-highest score. Concerning CHB-MIT datasets, the proposed scheme with the DTree classifier also obtained the second-highest score.

Next, we evaluated the proposed model per user dataset in this study. Tables 4–7 report the classification results of the proposed method based on 10-cross validation. It can be observed that the proposed ORDWT_AR technique performed well with the WKNN classifier, achieving the highest accuracy with all the datasets. However, the proposed ORDWT_AR technique with the DTree classifier showed an acceptable performance. The DTree classifier obtained the second-highest classification accuracy.

In addition, the metrics f-score, precision, and recall were also employed to evaluate the proposed model. Fig. 6 shows the performance of the proposed model in terms of score, precision, and recall per user for all datasets. The proposed model achieved an average f-score, precision, and recall of 99 %, 98 %, and 99 %, respectively, from all the users for the IVa dataset, 98 %, 99 %, 98 % for the V dataset, 99 %, 98 %,97 % for IIIa dataset, and 98 %, 97 %, and 99 % for CHB-MIT.
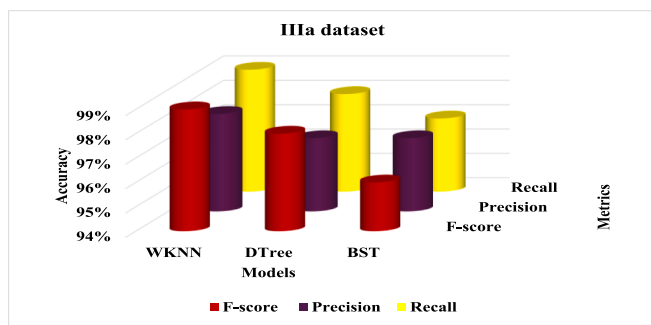
3.1. Performance evaluation using LOOCV metrics

For further assessment, Leave-One-Out Cross-Validation (LOOCV) metric was adopted. In this experiment, another EEG dataset which was collected from ttps://openbci.com/community/publicly-available-eeg-datasets/ 2024 was used to evaluate the proposed ORDWT_AR technique. A total of 20 subjects were collected and utilised for the performance evaluation. The EEG signals were collected using 64-channels based on the 10–10 Electrode system. Each subject was asked to do imagined moving their left hand or right hand. In this experiment, accuracy, f-score, recall, and precision were employed to evaluate the performance of the proposed. Fig. 7 reports the classification results, form the results obtained, we can notice that the proposed ORDWT_AR technique performed very well cross all subjects, however, the accuracy was dropped with subjects 20 and 17. Our findings showed that there were misclassifications to motor imagery right hand and left hand classes. Although there was slight fluctuation in the performance of the proposed mode, it obtained were acceptable results, and it performed very well cross most of subjects.

Table 4
Accuracy (%) of the proposed technique for MI EEG from the IVa datasets.

Database	Classifier	Accuracy %										Average
		F1	F2	F3	F4	F5	F6	F7	F8	F9	F10	
IVa datasets	WKNN	98	97	100	99	98	100	100	98	100	100	99
	DTree	98	97	98	98	99	98	97	98	98	99	98
	BST	98	98	97	91	99	96	97	98	97	96	96.7

Table 5
Accuracy (%) of the proposed technique for MI EEG from the V datasets.

Database	Classifier	Accuracy %										Average
		F1	F2	F3	F4	F5	F6	F7	F8	F9	F10	
V datasets	WKNN	100	99	100	100	100	99	100	99	100	100	99.7
	DTree	82	83	84	82	83	83	82	84	85	82	83
	BST	66	66	67	73	66	73	70	73	72	70	69.6

Table 6
Accuracy (%) of the proposed technique for MI EEG from the IIIa datasets.

Database	Classifier	Accuracy %										Average
		F1	F2	F3	F4	F5	F6	F7	F8	F9	F10	
	WKNN	99	99	100	98	100	99	100	99	100	99	99.3
IIIa datasets	DTree	99	98	99	99	98	99	99	99	99	98	98.7
	BST	98	99	99	98	97	99	98	99	99	98	98.4

Table 7
Accuracy (%) of the proposed technique for MI EEG from the CHB-MIT datasets.

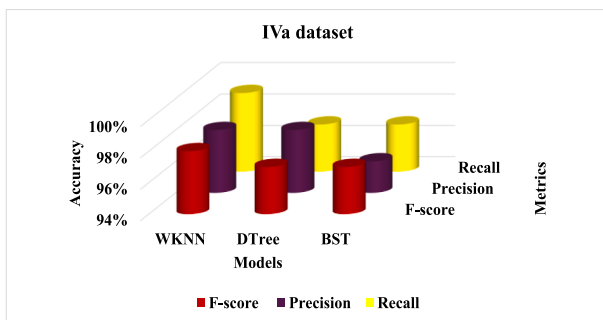| Database	Classifier	Testing										Average
		F1	F2	F3	F4	F5	F6	F7	F8	F9	F10	
	WKNN	99	99	100	98	100	99	100	99	100	99	99.3
CHB-MIT datasets	DTree	99	98	99	99	98	99	99	99	99	98	98.7
	BST	98	95	96	85	97	95	77	76	94	74	88.7

b. IIIa dataset
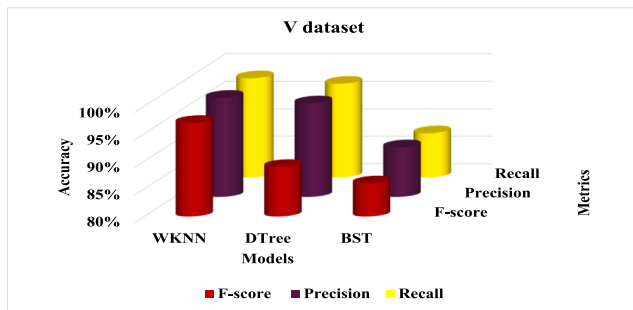
c. V dataset

d. V dataset

Fig. 6. Performance evaluation using f-score, recall and precision.

4. Discussion

The results obtained from the proposed ORDWT_AR method indicated noticeable improvements over the state of the art. The suggested model showed its effectiveness and ability to categorise motor tasks from EEG signals. In this section, the main findings are highlighted.

- For further analysis, this study examined the proposed ORDWT_AR method in terms of the overall accuracy rate (OAR) versus each fold, as shown in Fig. 8. From Fig. 8, it is observed that the ranges of the OAR from the ORDWT_AR technique were varied. The highest OAR was from the proposed method with the WKNN classifier for the EEG databases. The lowest OAR was from the BST classifier for all the tests. The experiment results demonstrated that the ORDWT_AR combined with the WKNN classifier was the best method to classify the BCI EEG recordings. The results in Fig. 8 support our findings in Tables 3–6.
- To validate the performance of the proposed ORDWT_AR model. The Friedman test (FT) was conducted in this paper. The number of classification models was 3, the number of EEG datasets was 4, and the significance level was set to 0.05 ($\alpha = 0.05$). The FT value should be less than the critical value. Otherwise, the null hypothesis will be rejected. Table 8 presents the significant and FT values regarding accuracy, precision, f-score, kappa, and recall. From the results, we can see that all FT values were greater than the significant value. We can conclude that all the compared models had substantial differences.
- The Receiver Operating Characteristics (ROC) curves were also employed for further evaluation. ROC curves are appropriate metrics to investigate the dependency of specificity and sensitivity. ROC curves describe the relationships among actual negative rate, false negative rate, and valid positive rate. Fig. 9 demonstrates the performance of three classification models using the ROC curves. It can be observed that the proposed ORDWT_AR combined with WKNN correctly classified most motor tasks.
- Another experiment was also conducted using the Hamming loss metric, which tests the fraction of misclassified motor takes. The value of the Hamming loss metric ranges from 1 to 0; the smaller the value indicates a good performance. The value 0 is the perfect value. Fig. 9 shows the performance of classification models in terms of Hamming loss. The results in Fig. 10 highlight the efficiency of the proposed ORDWT_AR model combined with WKNN against other models. The proposed ORDWT_AR model combined with WKNN gained the lowest HLO compared to other models.
- In addition, this study compared the proposed ORDWT_AR method with some recently reported studies (Wu et al., (2008), Lin and Hsieh (2009), Jin et al., (2019)) to assess its performance. Table 9 shows the comparison of the proposed approach with eleven other existing methods. From Table 9, Kevric and Subasi (2017) applied a wavelet packet decomposition to extract the key features based on the multiscale principal component analysis and higher-order statistics
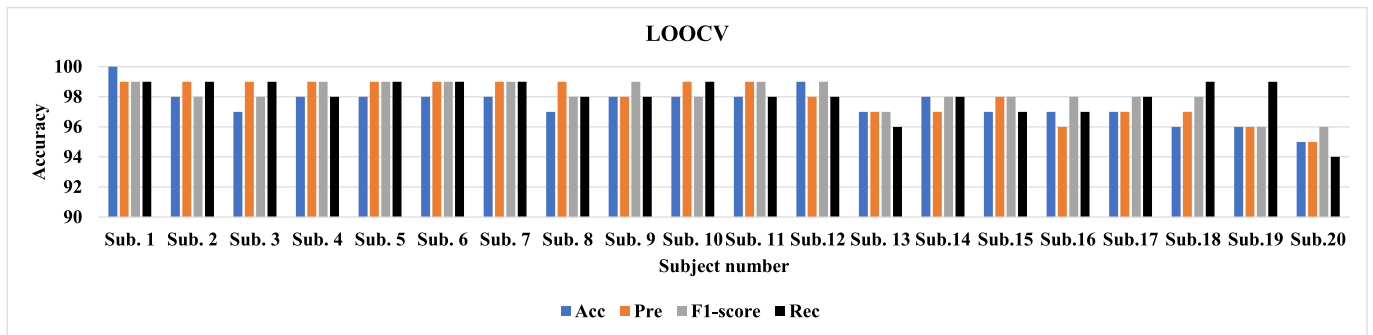
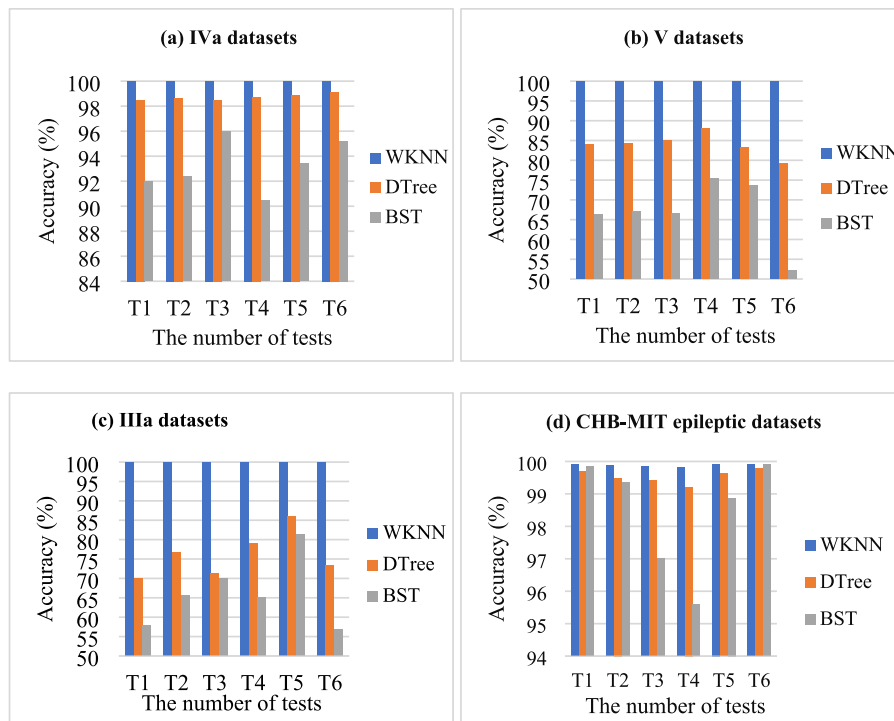**Fig. 7.** Performance evaluation using LOOCV metric.

Fig. 8. The OAR comparisons among the three classifiers with the ORDWT_AR technique for BCI Competition III and CHB-MIT epileptic datasets.

Table 8
Performance evaluation using the FF test.

Metric	FT	Significant value
Accuracy	99.548	
F-score	98.987	2.323
Recall	97.765	
Precision	98.876	
Kapp coefficient	96.654	

feature methods and classify the extracted features by a KNN classifier. They achieved an overall accuracy rate of 92.8 %. for the IVa database. However, our method obtained a 100 % overall accuracy rate for the three BCI Competition III EEG databases (IIIa, IVa and V datasets). Siuly et al. (2016) applied an optimum allocation technique with a Naïve Bayes classifier to classify the mental imagery-based EEG signals. In total, they yielded an average classification accuracy of 96.8 %. Siuly et al. (2011) developed a method that used cross-correlation and a logistic regression classifier. The researchers reported a 93.91 % classification accuracy for IVa EEG datasets in BCI Competition III. Another study was made by Siuly et al., (2016)

that applied two different methods individually to classify the IVa and V databases. The two methods were clustering and simple random sampling with a least square support vector machine classifier. As seen in Table 9, the proposed scheme achieved a higher accuracy than Siuly et al.'s (2014). Wu et al. (2008) yielded a 94.21 % average accuracy for the IVa database using an iterative spatio-spectral pattern learning method. Lin and Hsieh (2009) reported a method based on an improved particle swarm optimisation combined with a neural network to classify the V datasets from the mental imagery EEG data. That method gained a 68.35 % classification rate. In comparison, our ORDWT_AR technique yielded 100 % accuracy for the same database. She et al. (2018) developed a novel method, which is a common spatial pattern mixture with fisher discrimination criterion. They also applied an extreme learning machine to classify the EEG-extracted features. They achieved 80.68 % and 87.54 % accuracy rates for datasets IVa and IIIa in BCI Competition III EEG databases, respectively. Furthermore, the proposed method also gained higher OAR than that of their approach, as shown in Table 9. Selim et al. (2020) obtained 85 % and 86.6 % classification accuracy for datasets IVa and IIIa in BCI Competition III databases by applying a new method. They utilised a typical spatial
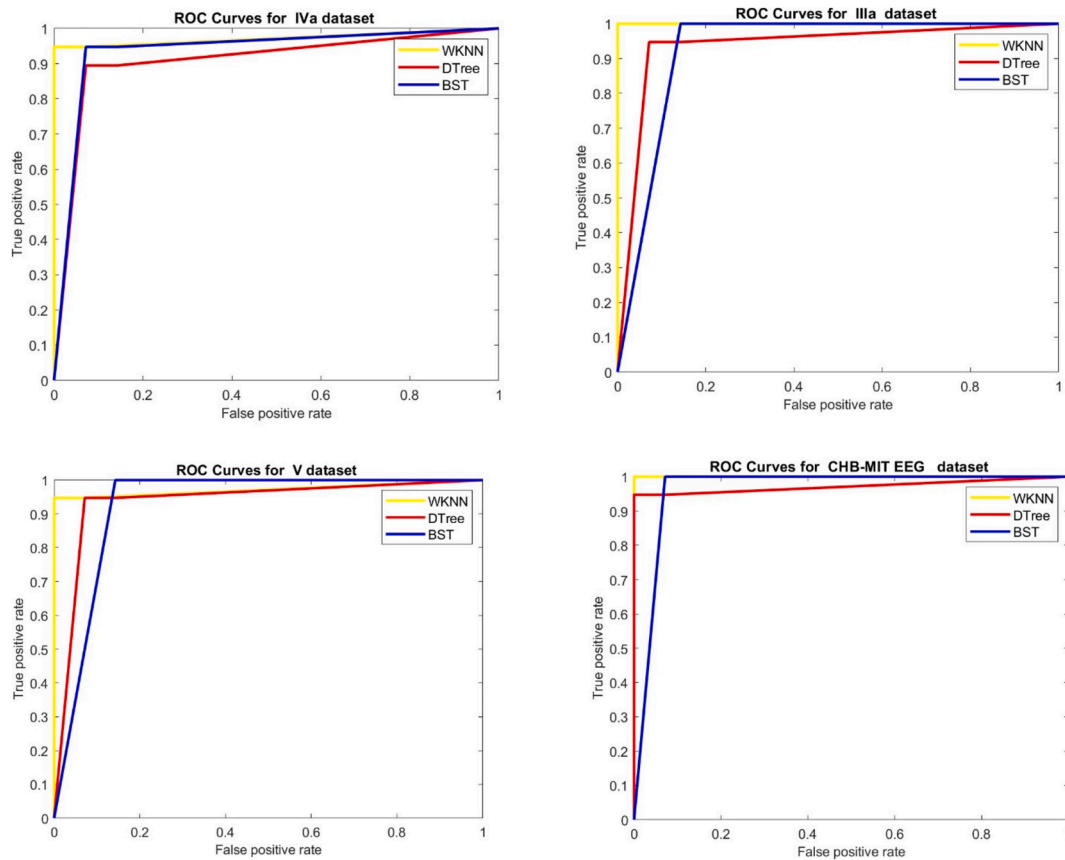
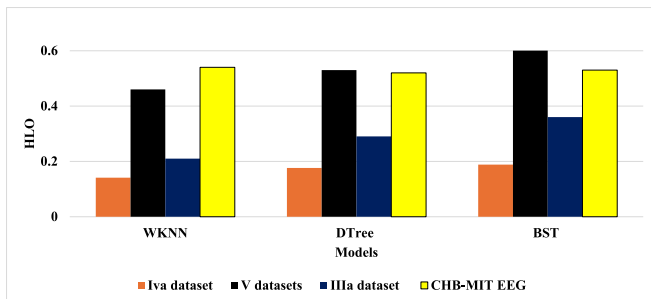**Fig. 9.** The ROC curves for four datasets.

Fig. 10. Performance evaluation hlo metric.

pattern (CSP) to extract features from EEG signals. They used a hybrid attractor metagene and Bat optimisation to select the most discrimination-extracted features from CSP. A support vector machine was also employed to classify the EEG BCI Competition III system. Obviously, our technique was better than their method. In 2019, Jin et al. (2019) provided a new technique to classify motor imagery EEG signals. They implemented a correlation-based channel selection approach to select the channels with the most related information. They are also used to regularize a common spatial pattern to extract discriminative features. To classify the extracted features, they applied a support vector machine. Their method obtained 87.4 % and 91.9 % for IVa and IIIa EEG datasets, respectively, as seen in Table 9. Most recently, Selim et al. (2018) employed five feature extraction methods to choose the best approach for EEGs. They found that the common spatial pattern feature extraction technique based on linear discriminant analysis achieved the highest classification accuracy, with a 79.77 % accuracy for IVa datasets and 86.48 % for IIIa datasets. In the same year, Yu et al. (2020) used a new feature

extraction scheme based on phase-locking value combined with local temporal common spatial patterns. They obtained 83.25 % and 90.56 % for IVa and IIIa datasets, respectively, as shown in Table 9. Recently, Tiwari and Chaturvedi (2021) found an effective way to minimize the redundancy of EEG channels by using the dynamic channel relevance method. They achieved slightly more than 85 % for dataset IVa. Meanwhile, Phadikar et al. (2023) developed an unsupervised neural network using the weight vector of the autoencoder. They also applied rectangular windowing to extract the representative features. Their method obtained 95.33 % for dataset IIIa. Most existing methods were conducted using the IVa datasets, and overall classification accuracy was obtained between 76 % and 97 %. Some of those methods utilized the V datasets for their study and achieved an average accuracy between 60 % − 69 %. Furthermore, some researchers used IIIa datasets and yielded 86 % − 91 % classification accuracy compared with the proposed ORDWT_AR scheme that used three different datasets from BCI Competition III (IIIa, IVa and V). Table 9 highlights the best result among all the techniques in bold font. The proposed ORDWT_AR scheme with the WKNN classifier achieved the highest accuracy compared to other methods.

- In addition, this research also compared the proposed approach using the CHB-MIT datasets with several recent reported research, as shown in Table 10. Table 10 summarizes the performance comparison between the proposed and state-of-the-art methods. Compared with the reported results from (Xiang et al., 2025), Bhattacharyya and Pachori (2017), Jiang et al., (2020), Liu et al., (2022), Xiong et al. (2022). The accuracy of the proposed ORDWT_AR technique was slightly the highest. The proposed scheme can deal with large amounts of data. The main limitation of the proposed method is that it may cause a little delay for real-time applications due to the feature extraction procedure.

Table 9

The OAR comparison between the proposed scheme and other existing methods using three BCI EEG databases.

Researcher	Method	Database	OAR (%)
Kevric and Subasi (20117)	Multiscale principal component analysis + wavelet packet decomposition + higher order statistics features + KNN classifier	IVa	92.8
Siuly et al., (2016)	Optimum allocation + Naïve Bayes classifier	IVa	96.36
Siuly et al., (2011)	Cross correlation + Logistic regression classifier	IVa	93.91
Siuly et al., [43]	Clustering technique + Least square support vector machine	IVa V	84.17 61.69
	Simple random sampling + Least square support vector	IVa V	76.71 60.15
Wu et al., (2008)	Iterative spatio-spectral patterns learning	IVa	94.21
Lin and Hsieh (2009)	Improved particle swarm optimisation + neural network classifier	V	68.35
She et al., (2018)	A common spatial pattern + Fisher discrimination criterion + extreme learning machine	IVa IIIa	80.68 87.54
Selim et al., (2020)	A common spatial pattern + A hybrid attractor metagene and the Bat optimisation + Support vector machine	IVa IIIa	85.0 86.6
Jin et al., (2019)	A correlation-based channel + A regularized common spatial pattern + Support vector machine	IVa IIIa	87.4 91.9
Selim et al., (2018)	A common spatial pattern + linear discriminant analysis	IVa IIIa	79.77 86.48
Yu et al., (2020)	Phase-locking value + local temporal common spatial patterns	IVa IIIa	83.25 90.56
Tiwari and Chaturvedi (2021)	Dynamic Channel Relevance + Support vector machine	IVa	85.20
Phadikar et al., (2023)	Weight vector of autoencoder + Rectangular windowing + Support vector machine	IIIa	95.33
The proposed scheme	**−ORDWT_AR + WKNN**	**IVa** **V** **IIIa**	**99** **99.7** **99.3**

Table 10

The OAR comparison between the proposed scheme and other existing methods using epileptic CHB-MIT dataset.

Researcher	Method	OAR (%)
Xiang et al., (2025)	Fuzzy entropy + K-S test + support vector machine	98.31
Bhattacharyya and Pachori (2017)	Empirical wavelet transform + random forest	99.57
Yuan et al., (2018)	Unified multi-view deep learning	94.37
Wu et al., (2019)	feature extraction + random forest classification	99.36
Jiang et al., (2020)	Symplectic geometry decomposition + support vector machine	99.62
Zhang et al., (2020)	Differential entropy + row and column attention with a shallower VGGNet	95.12
Liu et al., (2022)	Wavelet decomposition + Convolutional neural network + Bidirectional long short-term memory	97.51
Xiong et al. (2022)	Multilayer network + Improved genetic algorithm + Random Forest	97.26
The proposed scheme	**−ORDWT_AR + WKNN**	**99.3**

- Although the proposed motor task identification gained acceptable accuracy, evaluating the proposed model with a big real EEG dataset is necessary to assess its robustness. In addition, other models, including ensemble classification models and feature selection

models, will be combined with the proposed ORDWT_AR technique to improve its performance.

5. Conclusion

Developing a novel method to analyse and classify EEG signal types from BCI interactions is critical. It can help disabled people to communicate outside of their world. Extracting discriminative features from a vast amount of EEG data is very important to accurately classify EEG recordings. This study developed a novel feature extraction technique for EEG classification. The over-complete rational dilation wavelet transform combined with the autoregressive model, named the ORDWT_AR technique, was applied for the feature extraction. The three popular WKNN, DTree and BST classifiers were tested to select the best classifier. The experiments were conducted using four publicly available benchmark EEG databases, two motor imagery (IIIa and IVa databases), and mental imagery tasks (V database) from BCI Competition III and CHB-MIT epileptic datasets, respectively. The experimental results showed that the proposed ORDWT_AR technique and the WKNN classifier efficiently classify the EEG signals. In the future, we will implement the ORDWT method with different power spectral models to extract features from large amounts of EEG recordings and improve efficiency.

Declaration of competing interest

The authors declare that they have no known competing financial interests or personal relationships that could have appeared to influence the work reported in this paper.

Data availability

The authors do not have permission to share data.

References

Abdulla, S., Diykh, M., Siuly, S., & Ali, M. (2023). An intelligent model involving multi-channels spectrum patterns-based features for automatic sleep stage classification. *International Journal of Medical Informatics, 171*, Article 105001.

Al-Hadeethi, H., Abdulla, S., Diykh, M., & Green, J. H. (2021). Determinant of covariance matrix model coupled with adaboost classification algorithm for EEG seizure detection. *Diagnostics, 12*(1), 74.

Alsafy, I., & Diykh, M. (2022). Developing a robust model to predict depth of anesthesia from single channel EEG signal. *Physical and Engineering Sciences in Medicine, 45*(3), 793–808.

Ang, K. K., Chua, K. S. G., Phua, K. S., Wang, C., Chin, Z. Y., Kuah, C. W. K., Low, W., & Guan, C. (2015). A randomized controlled trial of EEG-based motor imagery brain-computer interface robotic rehabilitation for stroke. *Clinical EEG and Neuroscience, 46*(4), 310–320.

Bayram, I. and Selesnick, I.W., 2007, October. Design of orthonormal and overcomplete wavelet transforms based on rational sampling factors. In *Wavelet Applications in Industrial Processing V* (Vol. 6763, pp. 127-141). SPIE.

Bayram, I., & Selesnick, I. W. (2009). Frequency-domain design of overcomplete rational-dilation wavelet transforms. *IEEE Transactions on Signal Processing, 57*(8), 2957–2972.

Bhattacharyya, A., & Pachori, R. B. (2017). A multivariate approach for patient-specific EEG seizure detection using empirical wavelet transform. *IEEE Transactions on Biomedical Engineering, 64*(9), 2003–2015.

Chatterjee, R., Maitra, T., Islam, S. H., Hassan, M. M., Alamri, A., & Fortino, G. (2019). A novel machine learning based feature selection for motor imagery EEG signal classification in Internet of medical things environment. *Future Generation Computer Systems, 98*, 419–434.

Chen, B., Zhang, Z., Sun, C., Li, B., Zi, Y., & He, Z. (2012). Fault feature extraction of gearbox by using overcomplete rational dilation discrete wavelet transform on signals measured from vibration sensors. *Mechanical Systems and Signal Processing, 33*, 275–298.

Chunduri, V., Aoudni, Y., Khan, S., Aziz, A., Rizwan, A., Deb, N., Keshta, I., & Soni, M. (2024). Multi-Scale spatiotemporal attention network for neuron based motor imagery EEG classification. *Journal of Neuroscience Methods*, Article 110128.

Diykh, M., Abdulla, S., Deo, R. C., Siuly, S., & Ali, M. (2023). Developing a novel hybrid method based on dispersion entropy and adaptive boosting algorithm for human activity recognition. *Computer Methods and Programs in Biomedicine, 229*, Article 107305.

Diykh, M., Abdulla, S., Oudah, A.Y., Marhoon, H.A. and Siuly, S., 2021. A novel alcoholic EEG signals classification approach based on adaboost k-means coupled with

statistical model. In *Health Information Science: 10th International Conference, HIS 2021, Melbourne, VIC, Australia, October 25–28, 2021, Proceedings 10* (pp. 82-92). Springer International Publishing.

Dose, H., Møller, J. S., Iversen, H. K., & Puthusserypady, S. (2018). An end-to-end deep learning approach to MI-EEG signal classification for BCIs. *Expert Systems with Applications, 114,* 532–542.

Fei, S. W., & Chu, Y. B. (2022). A novel classification strategy of motor imagery EEG signals utilizing WT-PSR-SVD-based MTSVM. *Expert Systems with Applications, 199,* Article 116901.

Ganapathy, S., Mallidi, S. H., & Hermansky, H. (2014). Robust feature extraction using modulation filtering of autoregressive models. *IEEE/ACM Transactions on Audio, Speech, and Language Processing, 22*(8), 1285–1295.

Gaur, P., Pachori, R. B., Wang, H., & Prasad, G. (2018). A multi-class EEG-based BCI classification using multivariate empirical mode decomposition based filtering and Riemannian geometry. *Expert Systems with Applications, 95,* 201–211.

Han, Y., Wang, B., Luo, J., Li, L., & Li, X. (2022). A classification method for EEG motor imagery signals based on parallel convolutional neural network. *Biomedical Signal Processing and Control, 71,* Article 103190.

Jiang, Y., Chen, W., & Li, M. (2020). Symplectic geometry decomposition-based features for automatic epileptic seizure detection. *Computers in Biology and Medicine, 116,* Article 103549.

Jin, J., Miao, Y., Daly, I., Zuo, C., Hu, D., & Cichocki, A. (2019). Correlation-based channel selection and regularized feature optimization for MI-based BCI. *Neural Networks, 118,* 262–270.

Kevric, J., & Subasi, A. (2017). Comparison of signal decomposition methods in classification of EEG signals for motor-imagery BCI system. *Biomedical Signal Processing and Control, 31,* 398–406.

Kwok, H. K., & Jones, D. L. (2000). Improved instantaneous frequency estimation using an adaptive short-time Fourier transform. *IEEE Transactions on Signal Processing, 48* (10), 2964–2972.

Lafta, R., Zhang, J., Tao, X., Li, Y., Diykh, M., & Lin, J. C. W. (2018). A structural graph-coupled advanced machine learning ensemble model for disease risk prediction in a telehealthcare environment. *Big Data in Engineering Applications,* 363–384.

Lin, C. J., & Hsieh, M. H. (2009). Classification of mental task from EEG data using neural networks based on particle swarm optimization. *Neurocomputing, 72*(4–6), 1121–1130.

Liu, G., Tian, L., & Zhou, W. (2022). Patient-independent seizure detection based on channel-perturbation convolutional neural network and bidirectional long short-term memory. *International Journal of Neural Systems, 32*(06), Article 2150051.

Ma, W., Wang, C., Sun, X., Lin, X., Niu, L., & Wang, Y. (2023). MBGA-net: A multi-branch graph adaptive network for individualized motor imagery EEG classification. *Computer Methods and Programs in Biomedicine, 240,* Article 107641.

Ma, W., Xue, H., Sun, X., Mao, S., Wang, L., Liu, Y., Wang, Y., & Lin, X. (2022). A novel multi-branch hybrid neural network for motor imagery EEG signal classification. *Biomedical Signal Processing and Control, 77,* Article 103718.

Meng, X., Qiu, S., Wan, S., Cheng, K., & Cui, L. (2021). A motor imagery EEG signal classification algorithm based on recurrence plot convolution neural network. *Pattern Recognition Letters, 146,* 134–141.

Nguyen, T., Khosravi, A., Creighton, D., & Nahavandi, S. (2015). EEG signal classification for BCI applications by wavelets and interval type-2 fuzzy logic systems. *Expert Systems with Applications, 42*(9), 4370–4380.

Pan, H., Zhang, Y., Li, L., & Qin, X. (2024). A design and implementation of multi-character classification scheme based on motor imagery EEG signals. *Neuroscience, 538,* 22.

Phadikar, S., Sinha, N., & Ghosh, R. (2023). Unsupervised feature extraction with autoencoders for EEG based multiclass motor imagery BCI. *Expert Systems with Applications, 213,* Article 118901.

Rajan, J. J., & Rayner, P. J. (1996). Generalized feature extraction for time-varying autoregressive models. *IEEE Transactions on Signal Processing, 44*(10), 2498–2507.

Selim, S., Tantawi, M., Shedeed, H. and Badr, A., 2020, March. A comparative analysis of different feature extraction techniques for motor imagery based BCI system. In *The International Conference on Artificial Intelligence and Computer Vision* (pp. 740-749). Cham: Springer International Publishing.

Selim, S., Tantawi, M. M., Shedeed, H. A., & Badr, A. (2018). A csp\am-ba-svm approach for motor imagery bci system. *IEEE Access, 6,* 49192–49208.

She, Q., Chen, K., Ma, Y., Nguyen, T., & Zhang, Y. (2018). Sparse representation-based extreme learning machine for motor imagery EEG classification. *Computational intelligence and neuroscience, 2018*(1), Article 9593682.

Shoeb, A. H. (2009). *Application of machine learning to epileptic seizure onset detection and treatment (Doctoral dissertation).* Massachusetts Institute of Technology).

Siuly, S., Li, Y. and Wen, P., 2010, July. Analysis and classification of EEG signals using a hybrid clustering technique. In *IEEE/ICME International Conference on Complex Medical Engineering* (pp. 34-39). IEEE.

Siuly, S., Wang, H., & Zhang, Y. (2016). Detection of motor imagery EEG signals employing Naïve Bayes based learning process. *Measurement, 86,* 148–158.

Siuly, S., Li, Y., & Wen, P. P. (2011). Clustering technique-based least square support vector machine for EEG signal classification. *Computer Methods and Programs in Biomedicine, 104*(3), 358–372.

Siuly, S., Li, Y., & Wen, P. P. (2014). Modified CC-LR algorithm with three diverse feature sets for motor imagery tasks classification in EEG based brain–computer interface. *Computer Methods and Programs in Biomedicine, 113*(3), 767–780.

Tiwari, A., & Chaturvedi, A. (2021). A novel channel selection method for BCI classification using dynamic channel relevance. *IEEE Access, 9,* 126698–126716.

Venkatachalam, K., Devipriya, A., Maniraj, J., Sivaram, M., Ambikapathy, A., & Iraj, S. A. (2020). A Novel Method of motor imagery classification using eeg signal. *Artificial Intelligence in Medicine, 103,* Article 101787.

Wang, H., Yu, H., & Wang, H. (2022). EEG_GENet: A feature-level graph embedding method for motor imagery classification based on EEG signals. *Biocybernetics and Biomedical Engineering, 42*(3), 1023–1040.

Wolpaw, J. R., Birbaumer, N., McFarland, D. J., Pfurtscheller, G., & Vaughan, T. M. (2002). Brain–computer interfaces for communication and control. *Clinical Neurophysiology, 113*(6), 767–791.

Wu, D., Wang, Z., Jiang, L., Dong, F., Wu, X., Wang, S., & Ding, Y. (2019). Automatic epileptic seizures joint detection algorithm based on improved multi-domain feature of cEEG and spike feature of aEEG. *IEEE Access, 7,* 41551–41564.

Wu, W., Gao, X., Hong, B., & Gao, S. (2008). Classifying single-trial EEG during motor imagery by iterative spatio-spectral patterns learning (ISSPL). *IEEE Transactions on Biomedical Engineering, 55*(6), 1733–1743.

Xiong, Y., Dong, F., Wu, D., Jiang, L., Liu, J., & Li, B. (2022). Seizure detection based on improved genetic algorithm optimized multilayer network. *IEEE Access, 10,* 81343–81354.

Yu, Z., Ma, T., Fang, N., Wang, H., Li, Z., & Fan, H. (2020). Local temporal common spatial patterns modulated with phase locking value. *Biomedical Signal Processing and Control, 59,* Article 101882.

Yuan, Y., Xun, G., Jia, K., & Zhang, A. (2018). A multi-view deep learning framework for EEG seizure detection. *IEEE Journal of Biomedical and Health Informatics, 23*(1), 83–94.

Zhang, J., Wei, Z., Zou, J., & Fu, H. (2020). Automatic epileptic EEG classification based on differential entropy and attention model. *Engineering Applications of Artificial Intelligence, 96,* Article 103975.

Zhang, Y., Wang, Y., Jin, J., & Wang, X. (2017). Sparse Bayesian learning for obtaining sparsity of EEG frequency bands based feature vectors in motor imagery classification. *International Journal of Neural Systems, 27*(02), Article 1650032.